A note on estimating absolute cytosolic Ca2+ concentration in sensory neurons using a single wavelength Ca2+ indicator

Journal:	*Molecular Pain*
Manuscript ID	MPX-23-0141
Manuscript Type:	Methodology
Date Submitted by the Author:	11-Dec-2023
Complete List of Authors:	Higham, James; University of Cambridge, Department of Pharmacology Smith, Ewan; University of Cambridge, Department of Pharmacology Bulmer, David; University of Cambridge, Department of Pharmacology
Keywords:	Calcium imaging, Sensory neurons, Fluorescent calcium indicator, Fluo4
Abstract:	Ca2+ imaging is frequently used in the investigation of sensory neuronal function and nociception. In vitro imaging of acutely dissociated sensory neurons using membrane-permeant fluorescent Ca2+ indicators remains the most common approach to study Ca2+ signalling in sensory neurons. Fluo4 is a popular choice of single-wavelength indicator due to its brightness, high affinity for Ca2+ and ease of use. However, unlike ratiometric indicators, the emission intensity from single-wavelength indicators can be affected by indicator concentration, optical path length, excitation intensity and detector efficiency. As such, without careful calibration, it can be difficult to draw inferences from differences in the magnitude of Ca2+ transients recorded using Fluo4. Here, we show that a method scarcely used in sensory neurophysiology – first proposed by Maravall and colleagues (2000) – can provide reliable estimates of absolute cytosolic Ca2+ concentration ([Ca2+]cyt) in acutely dissociated sensory neurons using Fluo4. This method is straightforward to implement; is applicable to any high-affinity single-wavelength Ca2+ indicator with a large dynamic range; and provides estimates of [Ca2+]cyt in line with other methods, including ratiometric imaging. Use of this method will improve the granularity of sensory neuron Ca2+ imaging data obtained with Fluo4.

Short report

A note on estimating absolute cytosolic Ca^{2+} concentration in sensory neurons using a single wavelength Ca^{2+} indicator

James P Higham[1*], Ewan St John Smith[1], David C Bulmer[1]

[1]Department of Pharmacology, University of Cambridge, Tennis Court Road, Cambridge, UK, CB2 1PD

*Author for correspondence: jph87@cam.ac.uk

Acknowledgements

This work was supported by the Biotechnology and Biological Sciences Research Council.

Abstract

Ca^{2+} imaging is frequently used in the investigation of sensory neuronal function and nociception. *In vitro* imaging of acutely dissociated sensory neurons using membrane-permeant fluorescent Ca^{2+} indicators remains the most common approach to study Ca^{2+} signalling in sensory neurons. Fluo4 is a popular choice of single-wavelength indicator due to its brightness, high affinity for Ca^{2+} and ease of use. However, unlike ratiometric indicators, the emission intensity from single-wavelength indicators can be affected by indicator concentration, optical path length, excitation intensity and detector efficiency. As such, without careful calibration, it can be difficult to draw inferences from differences in the magnitude of Ca^{2+} transients recorded using Fluo4. Here, we show that a method scarcely used in sensory neurophysiology – first proposed by Maravall and colleagues (2000) – can provide reliable estimates of absolute cytosolic Ca^{2+} concentration ($[Ca^{2+}]_{cyt}$) in acutely dissociated sensory neurons using Fluo4. This method is straightforward to implement; is applicable to any high-affinity single-wavelength Ca^{2+} indicator with a large dynamic range; and provides estimates of $[Ca^{2+}]_{cyt}$ in line with other methods, including ratiometric imaging. Use of this method will improve the granularity of sensory neuron Ca^{2+} imaging data obtained with Fluo4.

Findings

Background

Measuring changes in $[Ca^{2+}]_{cyt}$ is a commonly used method for determining the sensitivity of sensory neurons to different stimuli and investigating pro-nociceptive signalling pathways, with Fluo4 being a popular choice of single-wavelength Ca^{2+} indicator. As has been discussed in detail previously [1], one can estimate $[Ca^{2+}]_{cyt}$ from the optical properties of a fluorescent Ca^{2+} indicator using the following equation [2]

$$[Ca^{2+}]_{cyt} = K_D \frac{F - F_{min}}{F_{max} - F} \quad Equation\ (1)$$

Where K_D is the equilibrium dissociation constant for the binding of Ca^{2+} to the indicator (for Fluo4, this will be taken as 325 nM as estimates vary between 300 nM and 350 nM [1,3,4]; F is the measured emission intensity; F_{min} is the minimum emission intensity (usually found by lysing cells in a high concentration of a Ca^{2+} chelator in Ca^{2+}-free bath solution); and F_{max} is the maximum emission intensity (usually found by lysing cells in a high concentration of Ca^{2+}). Experimentally, it is difficult and impractical to measure F_{min} and F_{max} for the same set of cells because these measurements require cell lysis, and so F_{min} is often found in a parallel experiment (meaning that measures of F_{min} are made in different cells to those used to measure F and F_{max}). This problem can be circumvented if one considers Equation (1) in terms of the indicator's dynamic range ($R = F_{max}/F_{min}$), which yields

$$[Ca^{2+}]_{cyt} = K_D \frac{\frac{F}{F_{max}} - \frac{1}{R}}{1 - \frac{F}{F_{max}}} \quad Equation\ (2)$$

It is apparent that if R is large, as is the case for Fluo4 ($R \approx 85\text{-}100$ [1]), then 1/R will become negligible (as $1/R << F/F_{max}$), and Equation (2) can be rewritten as

$$[Ca^{2+}]_{cyt} = K_D \frac{\frac{F}{F_{max}}}{1 - \frac{F}{F_{max}}} \quad Equation\ (3)$$

The estimate of $[Ca^{2+}]_{cyt}$ provided by Equation (3) does not require the experimenter to find F_{min}. F_{max} can be found easily at the end of each experiment by applying 0.1% Triton-X in a bathing solution containing 10 mM Ca^{2+}. As R and K_D are properties intrinsic to the indicator, it is not necessary for them to be estimated for each experiment [1], though it is important to consider that these parameters are sensitive to the intracellular environment (e.g., pH, ionic composition) [5]. Therefore, adding a straightforward step to the end of each Ca^{2+} imaging experiment enables an estimate of $[Ca^{2+}]_{cyt}$ using Fluo4.

Estimating changes in $[Ca^{2+}]_{cyt}$

Ionomycin is often used to calibrate Ca^{2+} signals measured in sensory neurons and while this calibration provides some useful information, it cannot be used to estimate absolute $[Ca^{2+}]_{cyt}$. This is because ionomycin cannot raise $[Ca^{2+}]_{cyt}$ sufficiently to obtain a true F_{max} for the indicator. This is apparent if 50 mM KCl and 5 µM ionomycin are sequentially applied to sensory neurons in a bath solution containing 2 mM Ca^{2+} (Figure 1, trace *i*). Ionomycin application cannot have resulted in saturation of Fluo4 because the magnitude of Ca^{2+}

transients evoked by KCl (black traces) exceeded those evoked by ionomycin. Similar results were obtained after raising bath $[Ca^{2+}]$ to 20 mM during the application of ionomycin, though the response to ionomycin was greater under these conditions (Figure 1, trace *ii*).

While KCl is useful for identifying viable neurons, its use as a calibration for the magnitude of Ca^{2+} signals in sensory neurons is limited because the magnitude of the response to KCl relies on voltage-gated Ca^{2+} channel function and Ca^{2+} buffering, which may not be comparable between different sensory neuron subpopulations [6] or different experimental conditions.

The absolute F_{min} or F_{max} for Fluo4 – as with other indicators – can be found by applying 0.1% Triton-X (to lyse cells) with a high concentration of a Ca^{2+} chelator (1 mM EGTA) in Ca^{2+}-free bathing solution (Figure 2A, grey trace) or 10 mM Ca^{2+}-containing bathing solution (Figure 2A, black trace), respectively. The transient increase in F following the application of Triton-X/EGTA in Ca^{2+}-free bathing solution (Figure 2A, grey trace) represents liberation of Ca^{2+} from intracellular stores. It is important to note that in the case of Equation (3), as F tends towards F_{max}, $1 - F/F_{max}$ will tend towards zero and, hence, estimates of $[Ca^{2+}]_{cyt}$ become unreasonably large. While $F/F_{max} < 90\%$, F/F_{max} is approximately linear with $[Ca^{2+}]_{cyt}$ and provides a reliable measure of $[Ca^{2+}]_{cyt}$ (Figure 2B). Beyond 90%, F/F_{max} no longer provides a reliable metric of $[Ca^{2+}]_{cyt}$ and estimates become unreasonably large – as such, this has been dubbed the "zone of unreliability" (Figure 2B, red shaded region [7]). It is, therefore, important to ensure that F measured during an experiment remains within the approximately linear region of Equation (3) and does not exceed 90% F/F_{max}.

To test the utility of Equation (3) for measuring $[Ca^{2+}]_{cyt}$ in sensory neurons, 50 mM KCl was used to induce depolarisation-dependent Ca^{2+} transients (n = 33 neurons, 2 mM bath Ca^{2+}, Figure 2C). Estimates of $[Ca^{2+}]_{cyt}$ calculated using Equation (1) and Equation (3) were compared; the value for F_{min} used in Equation (1) was found in the experiment shown in Figure 2A. F_{max} was found for each neuron at the end of each experiment. The peak F evoked by KCl application remained below 90% of that evoked by Triton-X/10 mM Ca^{2+}; peak F/F_{max} was 0.72±0.02 (range: 0.45-0.87, Figure 2D). As such, reliable estimates of $[Ca^{2+}]_{cyt}$ are possible. Figures 2E and F show exemplar results from five neurons obtained using Equation (1) and Equation (3), respectively. The data look qualitatively very similar. The congruence in the estimates of $[Ca^{2+}]_{cyt}$ found using Equations (1) and (3) (Figure 2G) demonstrates that the dynamic range of Fluo4 is of sufficient magnitude to make its reciprocal negligibly small relative to F/F_{max}. The percentage error in the estimates of $[Ca^{2+}]_{cyt}$ provided by Equations (1) and (3) was lowest during the peak of the KCl-evoked Ca^{2+} transient (1.3±0.04%) and highest during baseline (3.3±0.2%, Figure 2H). No difference in the estimated average baseline $[Ca^{2+}]_{cyt}$ was found between Equations (1) and (3) ($p = 0.26$, Figure 2I). The estimates of peak $[Ca^{2+}]_{cyt}$ provided by Equations (1) and (3) were also no different ($p = 0.78$, Figure 2J). Importantly, estimates calculated from Equation (3) of both baseline (63.4±2.3 nM) and peak (956.9±88.1 nM) $[Ca^{2+}]_{cyt}$ agreed with previous estimates made using ratiometric Ca^{2+} imaging [8-11]. Changes in $[Ca^{2+}]_{cyt}$ evoked by 50 mM KCl are relatively large, but this method can also be used to calibrate smaller changes in $[Ca^{2+}]_{cyt}$. The application of the algogenic mediator bradykinin (BK, 250 nM, 2 mM bath Ca^{2+}) to sensory neurons raised $[Ca^{2+}]_{cyt}$ – calculated using Equation (3) – from 60.3±4.8 nM to 333.3±39.6 nM (n = 13 neurons, Figure 2K and L).

Basal $[Ca^{2+}]_{cyt}$

Multiple factors, including ageing [11] and inflammation [12], can affect basal $[Ca^{2+}]_{cyt}$ in rodent sensory neurons. We have examined the effect of soma size on resting $[Ca^{2+}]_{cyt}$ in sensory neurons (Figure 3A; soma area distribution shown in *inset*). Neurons were parsed into subgroups by soma area (A): small ($A < 400$ μm^2, n = 86), medium ($400 < A < 1000$ μm^2, n = 129) and large ($A > 1000$ μm^2, n = 78). Although there was no difference in resting $[Ca^{2+}]_{cyt}$

between small- and medium-area neurons (73.0±3.8 nM vs 74.3±3.8 nM, $p > 0.99$, Figure 3B), basal $[Ca^{2+}]_{cyt}$ in large-area neurons (52.8±2.6 nM) was lower than both small- ($p = 0.0002$) and medium-area ($p < 0.0001$) neurons (Figure 3B). Average basal $[Ca^{2+}]_{cyt}$ across all neurons in this sample was 68.2±2.2 nM (n = 293 neurons from 3 independent DRG preparations), in agreement with previous estimates in rodent sensory neurons [8-14]. A modestly reduced resting $[Ca^{2+}]_{cyt}$ in large-diameter sensory neurons has been observed in rat [6], but corroborating observations in mouse sensory neurons are lacking. It is not immediately clear why large-area sensory neurons would exhibit a lower resting $[Ca^{2+}]_{cyt}$, though it could be due to more efficient $[Ca^{2+}]$ buffering. To test this possibility, another sample of neurons (n = 112 neurons from 3 independent DRG preparations) was stimulated with 50 mM KCl and the decay of evoked Ca^{2+} transients (expressed as the time constant for the decay of the transient) was analysed across different neuronal sizes. There was a modest negative correlation between soma area and time constant ($r = -0.26$, $p = 0.0061$, Figure 3C). KCl-evoked Ca^{2+} transients in small-area neurons exhibited a time constant of 13.0±1.2 s (n = 39), compared to 8.0±1.0 s (n = 23) in large-area neurons ($p = 0.0068$, Figure 3D). KCl-evoked Ca^{2+} transients in medium-area neurons exhibited an intermediate time constant (10.4±0.8 s, n = 50) which was indistinguishable from that in small- ($p = 0.25$) and large-area ($p = 0.26$) neurons (Figure 3D). The more rapid decay of KCl-evoked Ca^{2+} transients in large-area neurons (compared with small-area neurons) is consistent with a greater capacity for Ca^{2+} buffering [6].

In summary, the method put forward by Maravall and colleagues [1] provides a straightforward, easy-to-implement and – importantly – reliable protocol for estimating $[Ca^{2+}]_{cyt}$ in sensory neurons using a high dynamic range single-wavelength indicator without the need to estimate F_{min}. Estimates of $[Ca^{2+}]_{cyt}$ in sensory neurons made using this method with Fluo4 are well in-line with estimates made using other methods, including ratiometric Ca^{2+} imaging. F_{min} need not be estimated because the dynamic range of Fluo4 is sufficiently large, as evidenced by the close alignment of estimates of $[Ca^{2+}]_{cyt}$ between Equations (1) and (3). Use of this method broadens the utility of Fluo4 and will enable more rigorous quantification of Ca^{2+} signalling in sensory neurons using Fluo4.

Methods

Preparation of sensory neurons

All animal work was carried out in accordance with the Animals (Scientific Procedures) Act 1986. Mice (C57Bl/6, Charles River) were housed in groups of up to six littermates under a 12-hour light/dark cycle with bedding material, enrichment (e.g., igloos, tunnels, etc) and *ad libitum* access to food and water. All mice used were male aged 8-14 weeks.

Sensory neurons were prepared as described previously [15–17]. Briefly, dorsal root ganglia (DRG, T12-L5) were removed from the spinal column and enzymatically digested in collagenase (1 mg/mL) and trypsin (1 mg/mL). DRG were then mechanically dispersed by trituration through a pipette tip. Dispersed neurons were seeded onto glass-bottomed culture dishes coated with poly-D-lysine and laminin (MatTek, MA, USA). Neurons were incubated with supplemented L-15 growth medium (10% foetal bovine serum, 2.6% $NaHCO_3$, 1.5% D-glucose and 2% penicillin/streptomycin) at 37°C in 5% CO_2 and used for Ca^{2+} imaging no more than 24 hours after plating.

Ca^{2+} imaging

Growth medium was aspirated from culture dishes and neurons were incubated with 10 μM Fluo4-AM for 30-45 minutes at room temperature (shielded from light). Neurons were then washed and bathed in extracellular bath solution containing (in mM): 140 NaCl, 4 KCl, 2 $CaCl_2$, 1 $MgCl_2$, 4 D-glucose, 10 HEPES (pH 7.35-7.45 with NaOH; 290-310 mOsm). Ca^{2+}-free bath solution contained 2 mM $MgCl_2$. Dishes were mounted on an inverted Nikon Eclipse TE-2000S microscope and cells were visualised under brightfield illumination with a 10x air objective. Neurons were superfused with bath solution via a flexible inflow tube placed adjacent to cells of interest (AutoMate Scientific, CA, USA) fed by gravity-fed perfusion system (Warner Instruments, CT, USA).

All imaging was carried out at room temperature. Images were acquired at 2.5 fps with 100 ms exposure using a Retiga Electro CCD camera (QImaging, BC, Canada). Fluo4 was excited by a 470 nm light source (Cairn Research, UK) and emission at 520 nm was recorded using μManager [18]. For experiments using 50 mM KCl as a stimulus, KCl was superfused for 10s or 30 s following a 10 s baseline. For experiments using 250 nM bradykinin as a stimulus, bradykinin was superfused for 30 s following a 20 s baseline. At the end of all experiments, 0.1% Triton-X in 10 mM Ca^{2+} bath solution was superfused to lyse cells and yield an estimate for F_{max} for each neuron. F_{min} was estimated in one experiment by applying 0.1% Triton-X to neurons bathed in Ca^{2+}-free bath solution containing 1 mM EGTA.

Data analysis

Regions of interest were manually traced around neurons and the average pixel intensity per region per frame was calculated using ImageJ. After the subtraction of background fluorescence, measured fluorescence values for each neuron were calibrated to $[Ca^{2+}]$ using equations (1) and (3) using a K_D for Fluo4 of 325 nM.

Datasets were scrutinised to ensure that they met the assumptions of parametric analyses (normality tested using the Shapiro-Wilk test; equality of variances tested using F-tests) and, where appropriate, non-parametric, rank-based alternatives were used. Details of statistical tests used are in the figure legends. To find the time constant for the decay of KCl-evoked

Ca^{2+} transients, data were fit with a one-phase exponential decay. The time constant gives the time for the transient to decay by a factor of 1/*e*, i.e., ~37% of peak. This is equivalent to $T_{50}/ln(2)$, where T_{50} is the half-life of the decay of the transient, i.e., the time for the transient to decay by a factor of 0.5. Analysis was carried out in GraphPad Prism (GraphPad Inc.). Grouped data are displayed as mean ± standard error.

Figure legends

Figure 1

Calibration of Ca^{2+} transients using ionomycin.

Example traces showing the change in Fluo4 fluorescence over baseline (ΔF) during the application of 50 mM KCl and 5 μM ionomycin. KCl was applied in the presence of 2 mM bath Ca^{2+} (black traces), and ionomycin was applied in the presence of either 2 mM (blue trace) or 20 mM (orange trace) bath Ca^{2+}. In both cases, the peak fluorescence evoked by KCl application was greater than that evoked by ionomycin application, showing that ionomycin application cannot have resulted in saturation of the indicator.

Figure 2

Measuring changes in $[Ca^{2+}]_{cyt}$ in sensory neurons using Fluo4.

(A) Example traces from two neurons showing the application of 0.1% Triton-X to sensory neurons in the presence of either 10 mM bath Ca^{2+} (black trace) or 0 mM bath Ca^{2+} and 1 mM EGTA (grey trace). The peak of the orange trace shows F_{max} for this neuron, while the minimum of the purple trace shows F_{min}. The peak of the grey trace shows the liberation of Ca^{2+} from intracellular stores as the neuron is lysed.
(B) The relationship between F/F_{max} and $[Ca^{2+}]/K_D$. For $F/F_{max} < 90\%$, $[Ca^{2+}]/K_D$ remains small and approximately linear (*inset*). However, as F/F_{max} becomes larger (> 90%), estimates of $[Ca^{2+}]$ become unreliable (red shaded region).
(C) Example trace showing uncorrected Fluo4 fluorescence from a single neuron showing the application of 50 mM KCl (2 mM bath Ca^{2+}) and 0.1% Triton-X (10 mM bath Ca^{2+}).
(D) Example traces showing Fluo4 fluorescence normalised to F_{max} for five randomly-selected neurons during the application of 50 mM KCl. Traces in D-F are colour-coded to show data from individual neurons. *Inset*: grouped data showing peak F/F_{max} for all neurons imaged (n = 33 neurons from 3 independent DRG preparations, dashed line shows $F/F_{max} = 0.9$).
(E) Example traces showing $[Ca^{2+}]_{cyt}$ for five randomly-selected neurons during the application of 50 mM KCl. $[Ca^{2+}]_{cyt}$ was calculated from Equation (1) using $F_{min} = 5.852$ AU.
(F) Example traces showing $[Ca^{2+}]_{cyt}$ for five randomly-selected neurons during the application of 50 mM KCl. $[Ca^{2+}]_{cyt}$ was calculated from Equation (3).
(G) Scatterplot comparing estimates for $[Ca^{2+}]_{cyt}$ calculated using Equations (1) and (3) for the five neurons in D-F. Each dataset was fit with a straight line ($R^2 > 0.99$); the average slope was 1.006±0.0004 and each line passed approximately through the origin, showing a high congruence in the estimates of $[Ca^{2+}]_{cyt}$ provided by Equations (1) and (3).
(H) Heatmap showing the percentage error in the estimate of $[Ca^{2+}]_{cyt}$ between Equations (1) and (3) for each neuron (black bar shows KCl application).
(I) Grouped data showing the average baseline $[Ca^{2+}]_{cyt}$ calculated using Equations (1) and (3) for each neuron (n = 33 neurons from 3 independent DRG preparations). Data analysed using a Mann-Whitney U-test.
(J) Grouped data showing the peak $[Ca^{2+}]_{cyt}$ calculated using Equations (1) and (3) for each neuron (n = 33 neurons from 3 independent DRG preparations). Data analysed using a Mann-Whitney U-test.
(K) Example traces showing $[Ca^{2+}]_{cyt}$ (calculated using Equation [3]) during the application of 250 nM BK (13 neurons from 2 independent DRG preparations).

(L) Grouped data showing average baseline (pre-BK; mean of first 10 s of recording) and peak (post-BK) $[Ca^{2+}]_{cyt}$ (13 neurons from 2 independent DRG preparations).

Figure 3

Measuring basal $[Ca^{2+}]_{cyt}$ in sensory neurons parsed by soma size.

(A) Scatterplot showing soma size and average basal $[Ca^{2+}]_{cyt}$ (n = 293 neurons from 3 independent DRG preparations). *Inset*: frequency distribution of soma sizes.
(B) Grouped data showing the average basal $[Ca^{2+}]_{cyt}$ for small, medium and large sensory neuronal soma. Data analysed using a Kruskal-Wallis ANOVA with Dunn's post-hoc tests.
(C) Scatterplot showing soma size vs time constant for the decay of KCl-evoked Ca^{2+} transients (n = 112 neurons from 3 independent DRG preparations). Line of best fit shown to illustrate modest negative correlation (solid black line with 95% confidence limits shown as dashed lines). *Inset*: traces showing the decay of KCl-evoked Ca^{2+} transients in exemplar small- (orange), medium- (blue), and large-area (purple) neurons.
(D) Grouped data showing the time constant for KCl-evoked Ca^{2+} transients in small, medium and large sensory neuronal soma. Data analysed using a Kruskal-Wallis ANOVA with Dunn's post-hoc tests.

References

1. Maravall M, Mainen ZF, Sabatini BL, Svoboda K. Estimating intracellular calcium concentrations and buffering without wavelength ratioing. Biophys J. 2000;78.

2. Grynkiewicz G, Poenie M, Tsien RY. A new generation of Ca2+ indicators with greatly improved fluorescence properties. J. Biol. Chem. 1985.

3. Gee KR, Brown KA, Chen WNU, Bishop-Stewart J, Gray D, Johnson I. Chemical and physiological characterization of fluo-4 Ca2+-indicator dyes. Cell Calcium. 2000;27.

4. Kong W, Fast VG. The role of dye affinity in optical measurements of Cai2+ transients in cardiac muscle. Am J Physiol - Hear Circ Physiol. 2014;307.

5. Thomas D, Tovey SC, Collins TJ, Bootman MD, Berridge MJ, Lipp P. A comparison of fluorescent Ca2+ indicator properties and their use in measuring elementary and global Ca2+ signals. Cell Calcium. 2000;28.

6. Lu SG, Zhang X, Gold MS. Intracellular calcium regulation among subpopulations of rat dorsal root ganglion neurons. J Physiol. 2006;577.

7. Mammano F, Bortolozzi M. Ca2+ imaging: Principles of analysis and enhancement. Neuromethods. 2010.

8. Kim MS, Usachev YM. Mitochondrial Ca2+ cycling facilitates activation of the transcription factor NFAT in sensory neurons. J Neurosci. 2009;29.

9. Gemes G, Bangaru MLY, Wu HE, Tang Q, Weihrauch D, Koopmeiners AS, et al. Store-operated Ca2+ entry in sensory neurons: Functional role and the effect of painful nerve injury. J Neurosci. 2011;31.

10. Duncan C, Mueller S, Simon E, Renger JJ, Uebele VN, Hogan QH, et al. Painful nerve injury decreases sarco-endoplasmic reticulum Ca2+-ATPase activity in axotomized sensory neurons. Neuroscience. 2013;231.

11. Kirischuk S, Pronchuk N, Verkhratsky A. Measurements of intracellular calcium in sensory neurons of adult and old rats. Neuroscience. 1992;50.

12. Lu SG, Gold MS. Inflammation-induced increase in evoked calcium transients in subpopulations of rat dorsal root ganglion neurons. Neuroscience. 2008;153.

13. Shmigol A, Usachev Y, Pronchuk N, Kirishchuk S, Kostyuk P, Verkhratskii A. Properties of the caffeine-sensitive intracellular calcium stores in mammalian neurons. Neurophysiology. 1994;26.

14. Gemes G, Oyster KD, Pan B, Wu HE, Bangaru MLY, Tang Q, et al. Painful nerve injury increases plasma membrane Ca2+-ATPase activity in axotomized sensory neurons. Mol Pain. 2012;8.

15. Barker KH, Higham JP, Pattison LA, Taylor TS, Chessell IP, Welsh F, et al. Sensitization of colonic nociceptors by TNFα is dependent on TNFR1 expression and p38 MAPK activity. J Physiol. 2022;600.

16. Chakrabarti S, Pattison LA, Singhal K, Hockley JRF, Callejo G, Smith ESJ. Acute inflammation sensitizes knee-innervating sensory neurons and decreases mouse digging behavior in a TRPV1-dependent manner. Neuropharmacology. 2018;143.

17. Chakrabarti S, Jadon DR, Bulmer DC, Smith ESJ. Human osteoarthritic synovial fluid increases excitability of mouse dorsal root ganglion sensory neurons: An in-vitro translational model to study arthritic pain. Rheumatol (United Kingdom). 2020;59.

18. Edelstein AD, Tsuchida MA, Amodaj N, Pinkard H, Vale RD, Stuurman N. Advanced methods of microscope control using μManager software. J Biol Methods. 2014;1.

Figure 1

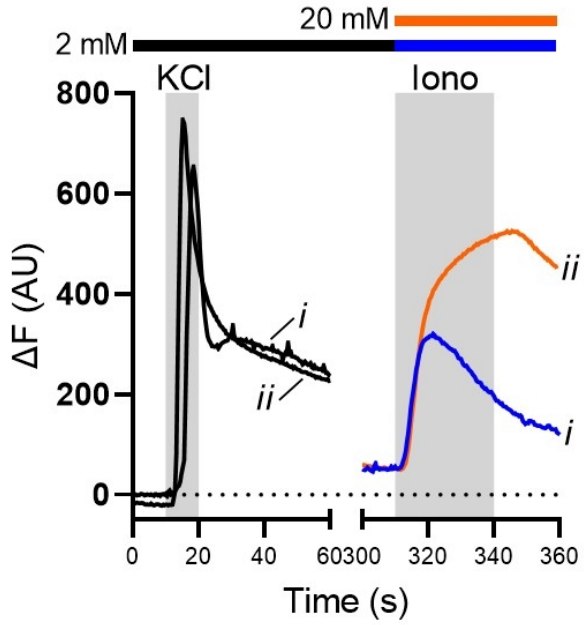

190x275mm (96 x 96 DPI)

Figure 2

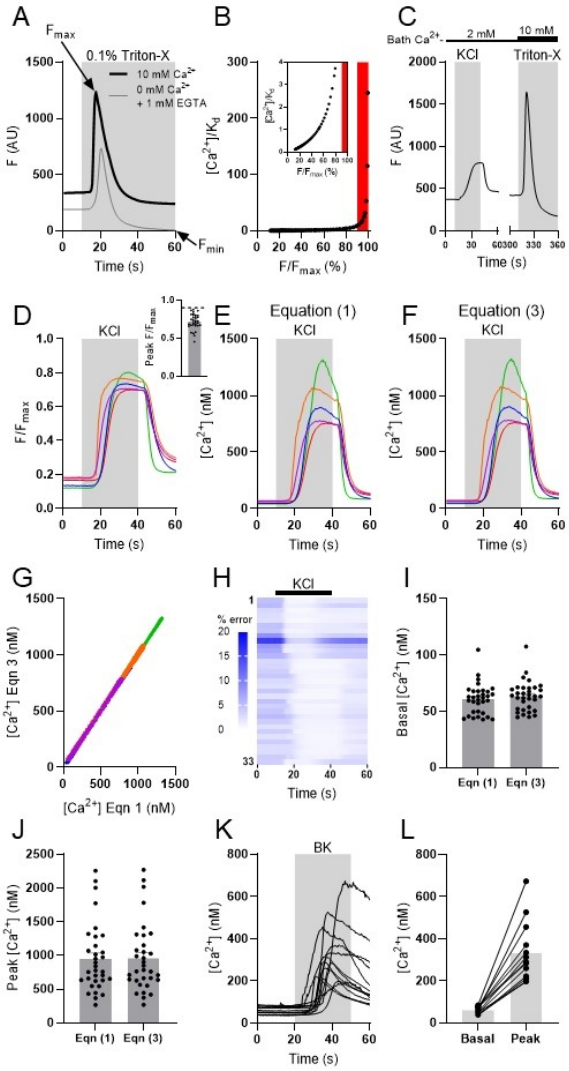

190x275mm (96 x 96 DPI)

Figure 3

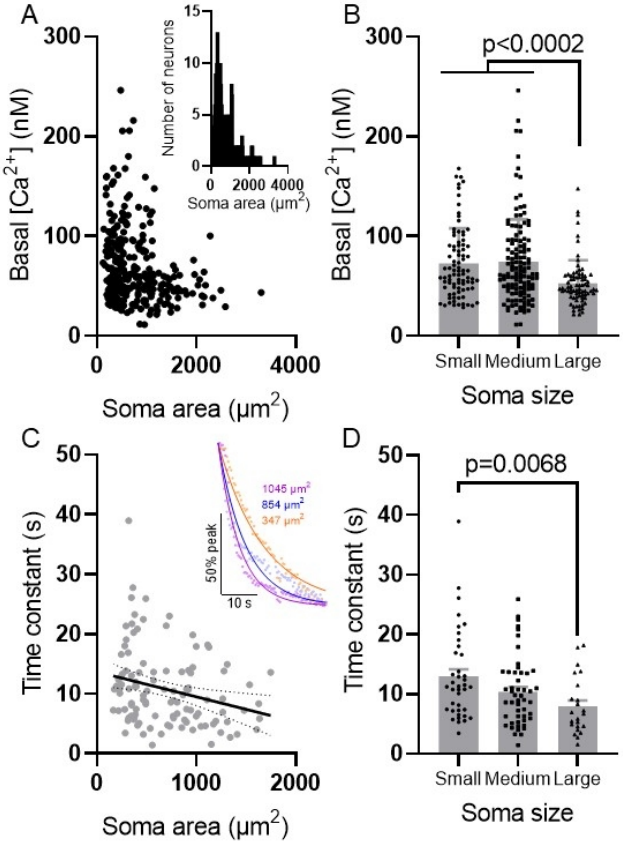

190x275mm (96 x 96 DPI)